Fatigue crack growth of aluminium alloy 7075-T651 under non-proportional mixed mode I and II loads

Xiaobo Yu
Aerospace Division, Defence Science and Technology Group, 506 Lorimer Street, Fishermans Bend, VIC 3207, Australia
xiaobo.yu@dsto.defence.gov.au, http://www.dsto.defence.gov.au

Ling Li, Gwénaëlle Proust
School of Civil Engineering, Faculty of Engineering & IT, the University of Sydney, NSW 2006, Australia
lili1626@uni.sydney.edu.au, gwenaelle.proust@sydney.edu.au

ABSTRACT. This study aims to investigate fatigue growth behaviour in AA7075-T651 under non-proportional mixed mode I and II loads. Fatigue tests were performed under cyclic tension and torsion using a thin-walled tubular specimen with a key-hole style crack starter. After the generation of a single-side mode I pre-crack, varied forms of mixed mode loads were applied, which in most cases led to a short distance coplanar growth followed by a long and stable crack path deviation. It was found that under most of the non-proportional mixed mode load cases, the direction of the deviated crack path could not be reasonably predicted using the commonly accepted maximum tangential stress criterion. Meanwhile, in some cases, the crack path directions could be approximately predicted using the maximum shear stress criterion. It was also confirmed for the first time that a long, stable and non-coplanar shear mode fatigue crack growth could be produced in AA7075-T651 under non-proportional mixed mode I and II loads. ©2016 Commonwealth of Australia

KEYWORDS. Fatigue crack growth; Non-proportional; Mixed mode; Aluminium alloy; 7075-T651.

Citation: Yu, X., Li, L. Proust, G., Fatigue crack growth of aluminium alloy 7075-T651 under non-proportional mixed mode I and II loads, Frattura ed Integrità Strutturale, 38 (2016) 148-154.

Received: 12.05.2016
Accepted: 15.06.2016
Published: 01.10.2016

INTRODUCTION

Fatigue of aircraft structures is traditionally managed based on the assumption of uniaxial loads. This is a simplified and acceptable approach for most fatigue critical locations where the local stress field is predominantly uniaxial due to loading path restrictions. Nevertheless, as evidenced in recent durability analysis of a new type of

surveillance aircraft, severe multiaxial loads may exist at some of the primary structural locations. Multiaxial fatigue analysis, including fatigue crack growth (FCG) analysis under non-proportional mixed mode I and II loads, is needed for these locations.

At present, experimental FCG investigations are predominantly undertaken for mode I or proportional mixed mode loads. Only a few studies [1-8] focus on non-proportional mixed mode loads. Limited results on A106-93 mild steel [3] reveal that a long and stable shear mode FCG – which is significantly different from the commonly understood open mode FCG – could be produced by non-proportional loads. To illustrate this difference, Fig. 1 compares the FCG behaviour under two load cases: (i) proportional load case TD1, under which, the FCG deviated into a direction that can be approximately predicted by the maximum tangential stress (MTS) criterion [9], and striations were found along the deviated crack path; (ii) non-proportional load case TD2, under which the FCG deviated to a direction that is about 60° off the MTS prediction, and dimples were found along the deviated crack path. For this particular case, the deviation angle is approximately predictable by the maximum shear stress (MSS) criterion [10].

The shear mode FCG as shown in Fig. 1 (d) is more than 8mm long along the deviated path. Thus, it is not a short-distance propagation in shear mode occurring in an early stage of crack growth as discussed in [7]. Nor is it a transient behaviour occurring at a short-distance coplanar growth following the change of load mixture as reported in [11]. The persistence of the shear mode FCG as presented in Fig. 1 (d) indicates the complexity of underlying mechanism under non-proportional loads. It means that a stage II fatigue crack can propagate in other than open mode growth, and in such a case, the crack path is absolutely unpredictable by the commonly accepted MTS criterion. Nevertheless, the above finding is so far only based on experimental results for A106-93 mild steel. It is not clear whether this finding also applies to other materials, such as aluminium alloy (AA) 7075-T651, which is typically used for aircraft structures, as no similar tests have been reported for the latter in the open literature.

Hence, the purpose of this study is to investigate FCG behaviour in AA7075-T651 under non-proportional mixed mode I and II loads. In particular, it aims to clarify whether the long and stable shear mode FCG also occurs. For the sake of comparison, the specimen design and majority of the mixed-mode load cases used in the present study are the same as reported in [3].

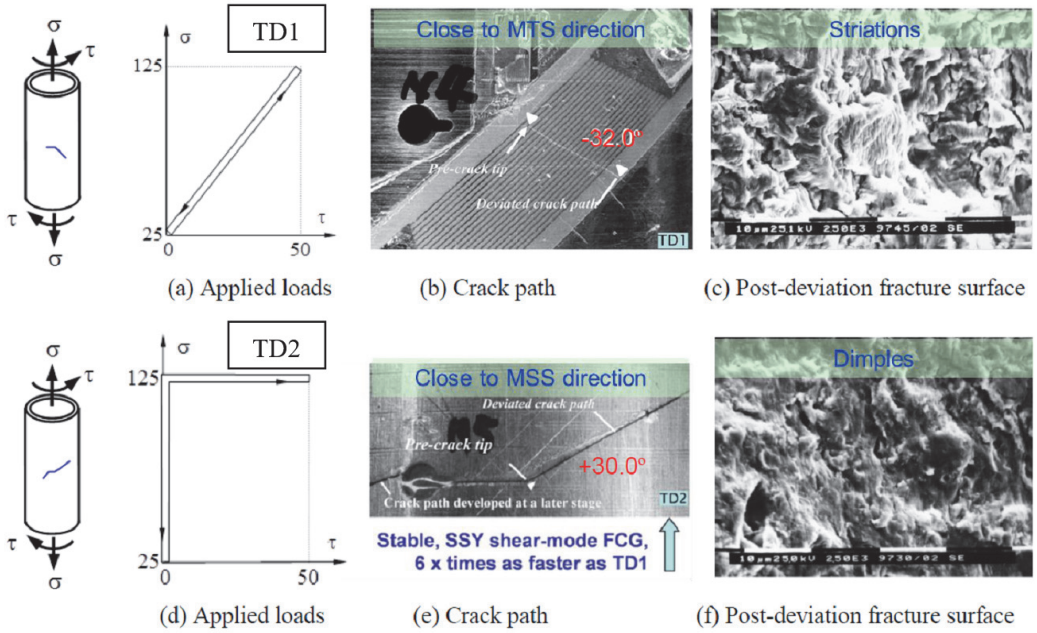

Figure 1: FCG from a mode I pre-crack, under proportional (a-c), and non-proportional (d-f), mixed-mode loads [3, 12]. (SSY in the figure refers to small scale yielding).

SPECIMEN AND TEST PROCEDURES

The fatigue tests of the present study were performed on an Instron 8500 servo-hydraulic tension-torsion biaxial fatigue test machine with a capacity of ±250 KN and ±2000 Nm. The test machine is located in the Structural Laboratory, School of Civil Engineering at the University of Sydney. This is the same test machine as the one that

was used in [3], except that the electronic test controllers have been upgraded prior to the present study.
The design of the specimen is the same as previously used in [3]. A schematic illustration of the specimen is given in Fig. 2, which includes a notched thin-walled tube and two solid plugs. Both the tube and plugs were machined from 2.5" AA7075-T651 solid bars, and the tight tolerance between the plugs and the tube was filled with Araldite epoxy adhesive. The plugs are reusable and their main function is to provide support to the tube under hydraulic grippers. The tube has a large diameter-to-thickness ratio of 38, which helps to suppress the effects of uneven shear stress distribution through the thickness. The crack starter notch has a keyhole shape, and was introduced via drilling and electronic discharge machining.

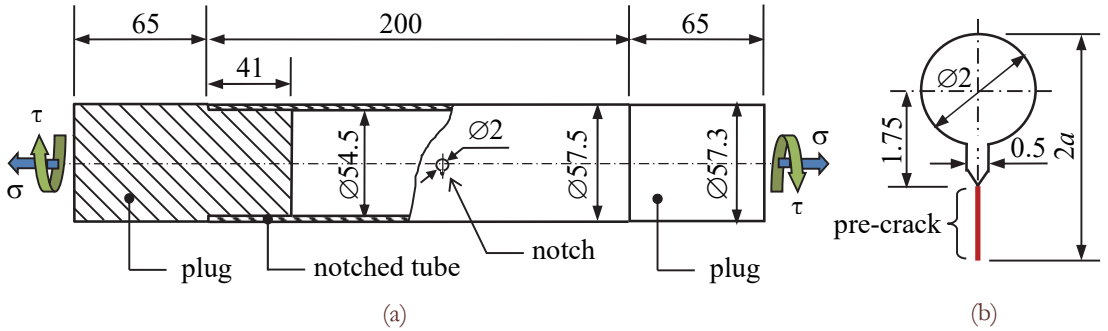

Figure 2: (a) Illustration of a tubular specimen for FCG test under cyclic tension and torsion. (b) The crack start notch with a single-sided mode I pre-crack. (after [3]).

The tension and torsion loads are described using σ and τ, which are the nominal tensile and shear stresses in an uncracked and un-notched tube. The positive direction of σ and τ, are shown in Fig. 2(a).
Ten specimens were tested. For each specimen, the fatigue test was performed in two phases. During phase 1 of the test, only tension was applied which cycled at 10Hz between 25 MPa and 125 MPa. A single-sided circumferential crack, here noted as pre-crack and illustrated in Fig. 2(b), was produced. The phase 1 procedure completed when the total crack length, 2a, reached between 7.5mm and 9mm approximately.
During phase 2 of the test, both tension and torsion were applied according to the τ-σ curves as illustrated in Fig. 3. The time-histories of tension and torsion feedback were monitored, and when needed load frequency was reduced to around 2Hz, to ensure that the target shape of the τ-σ curve was achieved. Each specimen was subject to a single load case, except for one specimen where three load cases (LC8, 9 and 10) were applied in a sequential order. At the pre-crack tip, the applied σ and τ produce mode I and mode II stress intensities, respectively, when the crack is fully opened. Strictly speaking, load cases LC1 to LC4 should be catalogued as proportional mixed mode loads. Nevertheless, they are here included for comparison. It is noted that all the load cases, except LC13, have been previously tested for A106-93 mild steel [3], and that the load cases LC4 and LC5 depicted in Fig. 3 are identical to TD1 and TD2 in Fig. 1.
All the fatigue tests were performed at room temperature in the laboratory environment. Fatigue crack growth was monitored using a portable optimal microscope and still images were taken at given intervals of cycles.

RESULTS AND ANALYSIS

For all ten specimens, the fatigue cracks produced by the end of the tests are shown in Fig. 4. These images were taken at the outer surface of the tubular specimens while the cracks were kept open under applied load in the test machine. The main interest here is the FCG behaviour under mixed mode loads, in particular the crack directions, as defined in Fig 4. Tab. 1 compares the measured crack directions with those predicted by the MTS [9] and MSS [10] criteria, which are expressed in Eqs. 1 and 2, respectively:

$$\text{MTS criterion:} \quad \frac{\partial \Delta\sigma_{\theta\theta}}{\partial\theta}=0 \ \text{ and } \ \frac{\partial^2 \Delta\sigma_{\theta\theta}}{\partial\theta^2}<0 \tag{1}$$

$$\text{MSS criterion:} \quad \frac{\partial \Delta\tau_{r\theta}}{\partial\theta}=0 \ \text{ and } \ \frac{\partial^2 \Delta\tau_{r\theta}}{\partial\theta^2}<0 \tag{2}$$

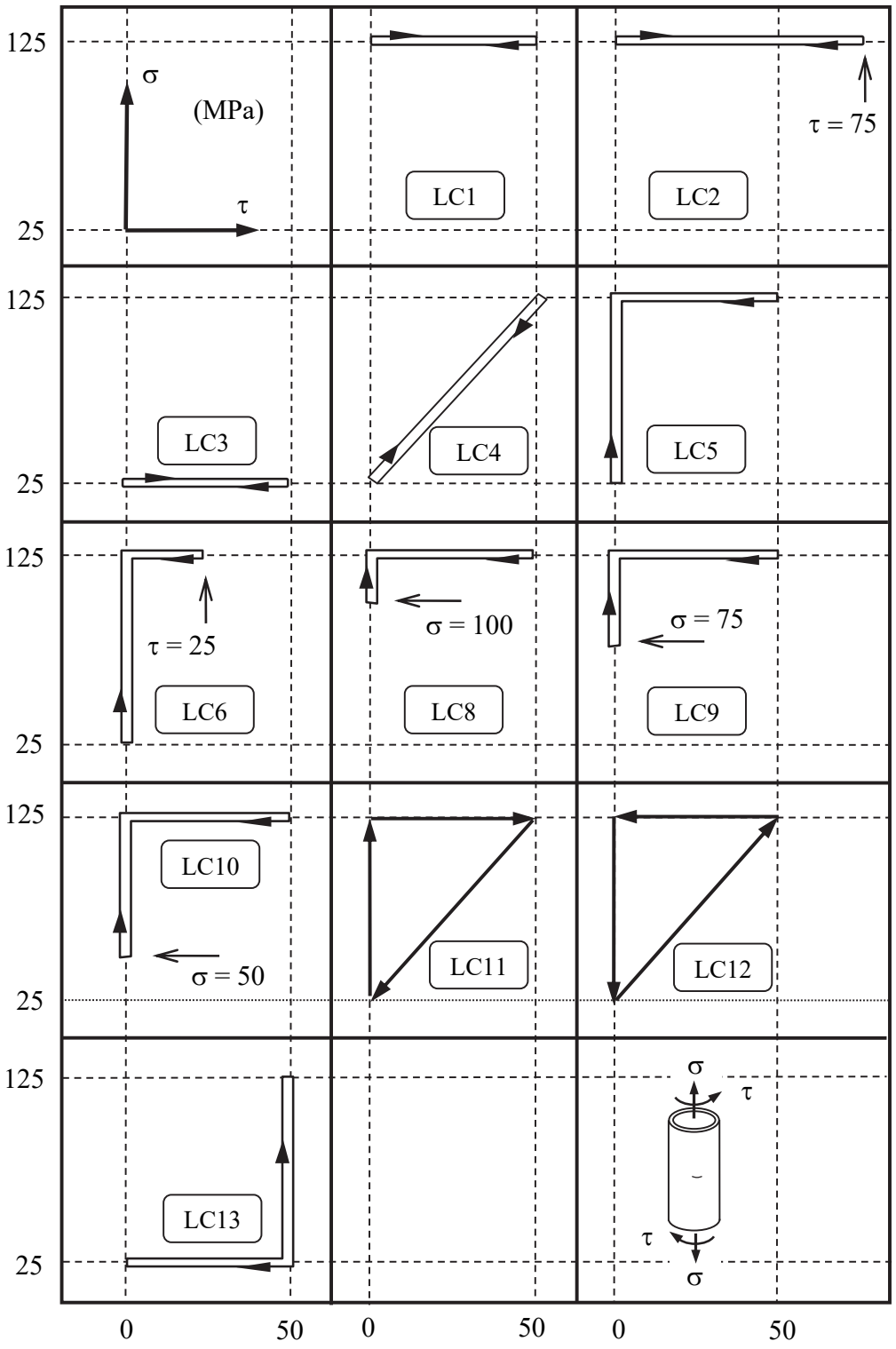

Figure 3: Load cases applied during the phase 2 of the fatigue tests.

Load Case	Pre-crack length (mm)	Coplanar FCG before branching		Crack direction (θ)		
		Length (mm)	Cycle	As measured	MTS criterion	MSS criterion
LC1	8.3	1.3	3200	-66.1°	**-70.5°**	0°
LC2	7.8	4.5	1850	+10.1°	-70.5°	**0°**
LC3	8.3	no growth	n/a	n/a	-70.5°	0°
LC4	8.1	0.54	650	-27.3°	**-40°**	+28.5°
LC5	8.0	0.4	750	+41°	-40°	**+28.5°**
LC6	8.4	0	411	+8°	-25.5°	+44°
LC8	7.5	0.6	4928	-52.5°	**-61.5°**	+8°
LC11	7.7	0.4	1832	+18.4°	-40°	**+28.5°**
LC12	9.1	0.8	568	-43.2°	**-40°**	+28.5°
LC13	8.3	0.3	1500	-19.9°	-40°	+28.5°

Table 1: Fatigue crack growth behaviour under mixed mode loads.

where, $\sigma_{\theta\theta}$ and $\tau_{r\theta}$ are tangential and shear stress calculated using Eq. 3 which is simplified from [13]. At the pre-crack tip, the mode I and mode II stress intensity factors were calculated as $K_I = \sigma\sqrt{\pi a}$ and $K_{II} = \tau\sqrt{\pi a}$, respectively. The effects of crack surface interference [14, 15] were not considered in this study.

$$\begin{Bmatrix}\sigma_{\theta\theta}\\ \sigma_{r\theta}\end{Bmatrix} = \frac{K_I}{\sqrt{2\pi r}}\cos\frac{\theta}{2}\begin{Bmatrix}\cos^2\frac{\theta}{2}\\ \sin\frac{\theta}{2}\cos\frac{\theta}{2}\end{Bmatrix} + \frac{K_{II}}{\sqrt{2\pi r}}\begin{Bmatrix}-3\sin\frac{\theta}{2}\cos^2\frac{\theta}{2}\\ \cos\frac{\theta}{2}(1-3\sin^2\frac{\theta}{2})\end{Bmatrix} \quad (3)$$

The results given in Tab. 1 shows that only four of the measured crack directions, or two of the six non-proportional load cases, can be approximately (with less than ±15° error) predicted using the MTS criterion. Meanwhile, three of the directions can be approximately predicted by the MSS criterion.

It is noted that the maximum and minimum values of σ and τ are all identical across five of the load cases, including LC4, 5, 11, 12 and 13. Nevertheless, the crack paths that were produced in the tests are all very different. The comparison between LC4 and LC5 is here elaborated. Under LC4 (proportional σ-τ variation), the crack path turns into a -27.3° direction, which is close to the MTS prediction. Meanwhile, under LC5 (non-proportional σ-τ variation), the crack path turns into a +41° direction, which is close to the MSS prediction. These two directions are more than 60° apart, showing the dependency of crack path, and hence the crack growth mechanism, on the relative phases between the σ and τ variations. A similar dependency was previously observed for A106-93 mild steel [3] as shown in Fig. 1. It means that for both the mild steel [3] and AA7075-T651 (this study), a long and stable shear mode FCG can be produced by applying non-proportional mixed mode load.

The comparison between LC11 and LC12 is also worth noting. For these two load cases, the τ-σ curves are the same except that one follows a clockwise direction, and the other follows an anti-clockwise direction. The crack paths as measured on the specimens are +18.4° and -43.2°, respectively, again more than 60° apart.

The load cases LC1, LC2 and LC3 tested here are similar to those achievable using a fixed-grip-shear specimens [16], where a static tensile (mode I) load was superimposed onto a cyclic shear (mode II) load. For the load case LC3 of the present study, no growth was observed from the pre-crack tip, which can be attributed to the severe crack closure and shear attenuation as the applied static tension is only one-fifth of the maximum σ applied during the pre-cracking phase. Under the load cases LC1 and LC2, nominal ΔK_{II} at the pre-crack tip were 5.7MPa·m$^{1/2}$ and 8.3MPa·m$^{1/2}$, respectively; and the FCG turned into -66.1° (close to MTS prediction) and +10.1° (close to MSS prediction) directions, respectively. It means that, under the cyclic τ plus static σ load conditions shear mode FCG can be produced under a higher ΔK_{II} for AA7075-T651. Similar observations were reported in [16] for AA7075-T6. However, under the same load case as LC2, no

shear mode FCG was observed for A106-93 mild steel [3]. This result reconfirms an earlier review finding [3] that under cyclic mode II loads, a shear mode FCG is more likely in aluminium alloys than in steels.

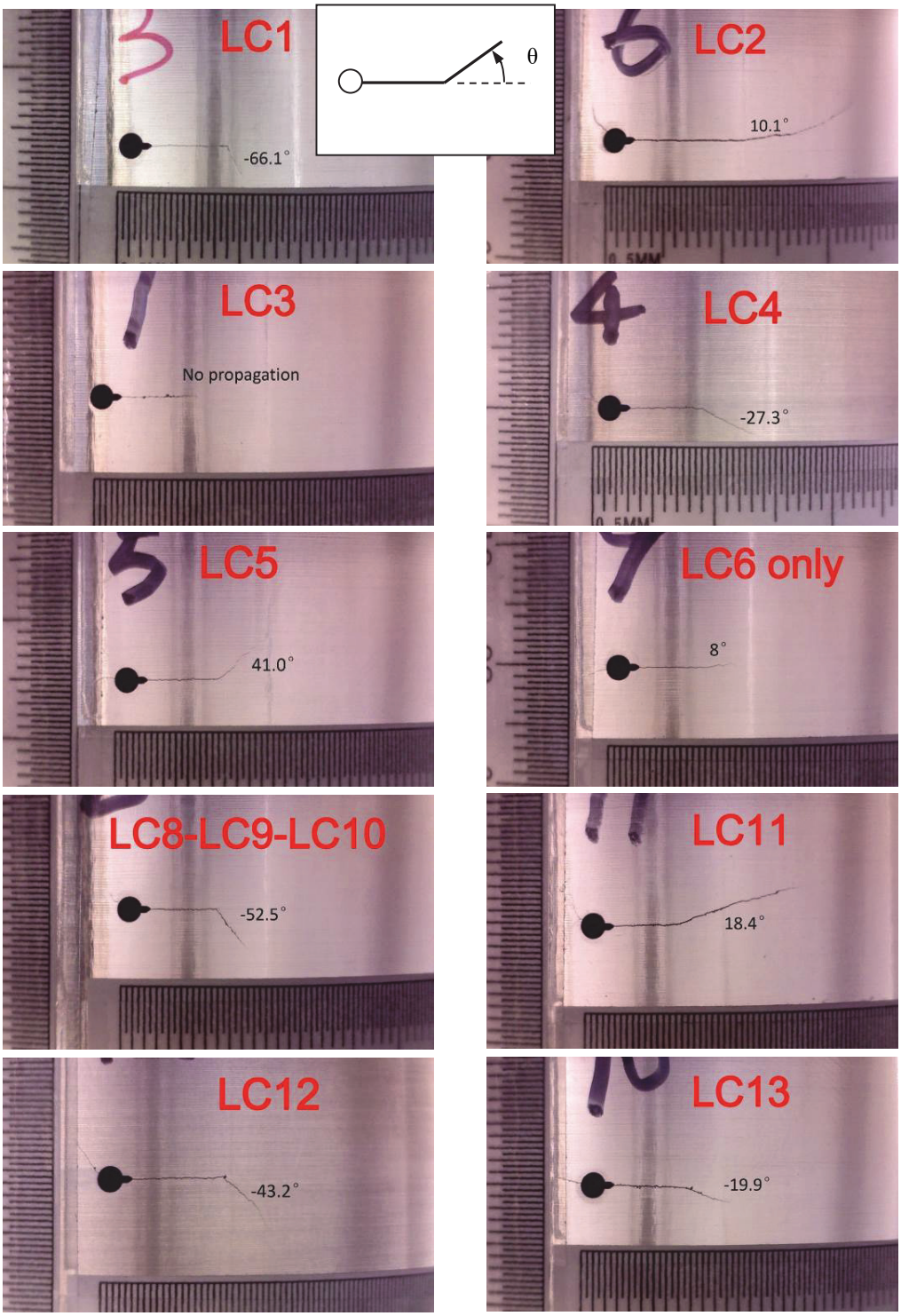

Figure 4: Fatigue cracks at the outer surface of tubular specimens at the end of tests.

Coplanar FCG was also observed under almost all load cases as summarised in Tab. 1. Nevertheless, for the loading cases where both σ and τ were cyclically applied, the coplanar growth was a transient behaviour, typically less than 1mm long, after which the FCG turned into the direction as discussed above.

It is noted that under most loading cases, a second crack also emanated from the far edge of the circular hole. However, the second crack only emerged after more than 4000 cycles of the applied mixed mode load. Therefore, their effect on crack path deviation was ignorable in this study.

CONCLUSION

This study clarifies that for AA7075-T651, the FCG under non-proportional mixed mode I and II loads is significantly different from the open mode FCG commonly expected under mode I or proportional mixed mode loads. Similarly to previous results for mild steel, a long and stable shear mode FCG can be produced in AA7075-T651 under non-proportional loads. The commonly accepted MTS criterion does not apply under most non-proportional load cases. Further investigations are needed to gain sufficient understanding, including those under in-service multiaxial loading spectra, to better support durability assessment of primary aircraft structures subjected to severe non-proportional multiaxial loads.

REFERENCES

[1] Nayeb-Hashemi, H., Taslim, M.E., Effects of the transient Mode II on the steady state crack growth in Mode I, Engng Fract Mech, 26(6) (1987) 789-807. doi:10.1016/0013-7944(87)90029-4.
[2] Wong, S.L., Bold, P.E., Brown, M.W., Allen, R.J., A branch criterion for shallow angled rolling contact fatigue cracks in rails, Wear, 191 (1-2) (1996) 45-53. doi: 10.1016/0043-1648(95)06621-7
[3] Yu, X., PhD thesis, the University of Sydney, Australia, (1999).
[4] Doquet, V., Pommier S., Fatigue crack growth under non-proportional mixed-mode loading in ferritic-pearlitic steel Fatigue Fract Engng Mater Struct, 27(11) (2004) 1051-1060. doi: 10.1111/j.1460-2695.2004.00817.x.
[5] Highsmith, S., Jr., PhD thesis, Georgia Institute of Technology, USA (2009).
[6] Doquet, V., Abbadi, M., Bui, Q. H., Pons, A., Influence of the loading path on fatigue crack growth under mixed-mode loading, Int J Fract, 159 (2009) 219-232. doi: 10.1007/s10704-009-9396-6.
[7] Shamsaei, N., Fatemi, A., Small fatigue crack growth under multiaxial stresses. Int J Fatigue, 58 (2014) 126–135. doi: 10.1016/j.ijfatigue.2013.02.002.
[8] Zerres, P., Vormwald, M., Review of fatigue crack growth under non-proportional mixed-mode loading, Int J Fatigue, 58 (2014) 75-83; doi: 10.1016/j.ijfatigue.2013.04.001.
[9] Erdogan, F., Sih, G.C., On the Crack Extension in Plates Under Plane Loading and Transverse ShearJ Basic Engng, 85(4) (1963) 519-525. doi:10.1115/1.3656897.
[10] Otsuka, A., Mori, K., Miyata T., The condition of fatigue crack growth in mixed mode conditions, Engng Fract Mech, 7(3) (1975) 429-439; doi:10.1016/0013-7944(75)90043-0.
[11] Smith, M.C., PhD thesis, University of Cambridge, UK, (1984).
[12] Yu, X., On the Fatigue Crack Growth Analysis of Spliced Aircraft Wing Panels under Sequential Axial and Shear Loads, Engng Fract Mech, 123 (2014) 116-125. doi: 10.1016/j.engfracmech.2014.03.018.
[13] Anderson, T.L. (1995) Fracture Mechanics: Fundamentals and Applications, 2nd Edition, CRC Press, Inc.
[14] Yu, X., Abel, A., Mixed-mode crack surface interference under cyclic shear loads, Fatigue Fract Engng Mater Struct, 23(2) (2000) 151-158. doi: 10.1046/j.1460-2695.2000.00236.x.
[15] Yu, X., Abel, A., Modelling of crack surface interference under cyclic shear loads, Fatigue Fract Engng Mater Struct, 22(3) (1999) 205-213; doi: 10.1046/j.1460-2695.1999.00152.x.
[16] Otsuka, A., Mori, K., Ohshima, T., Tsuyama, S., Mode II fatigue crack growth in aluminium alloys and mild steel, In: Advances in Fracture research, Fracture 81, ICF5, Francois, D. (Ed), (1981) 1851-1858.